Ring Resonator Optical Switches for Interconnection on Si Chips

Yuichiro Tanushi and Shin Yokoyama

Research Center for Nanodevices and Systems, Hiroshima University
1-4-2 Kagamiyama, Higashi-Hiroshima, Hiroshima 739-8527, Japan
Phone: +81-82-424-6265, Fax: +81-82-424-3499, E-mail: tanushi@sxsys.hiroshima-u.ac.jp

1. Introduction

Optical interconnection on Si chips is an attractive candidate for solving the signal delay of metal interconnection. Practical Si-based light-emitting devices have not been realized yet. We believe that a promising method is to integrate optical switches monolithically. We are studying tunable microring resonator for optical switches [1] because of their compactness (10-50 μm). In order to realize the ring resonator switches, the waveguide whose refractive index is changed by electric field is needed for high speed switching. There are two solutions to realize such waveguide: Electro-optic (EO) materials core waveguide and Si core waveguide [2]. Single-mode ring resonators have already been investigated [3, 4]. However, multimode waveguides are useful for short-distance interconnections because of their small propagation loss and small bending loss. We show that even multimode ring resonators have good resonance characteristics [5].

2. Ring Resonators using Silicon Nitride

Figure 1 shows the structure of multimode racetrack resonators with a waveguide width W, a radius R, a gap g, and a coupling length L. The core material of the waveguides is a silicon nitride (SiN) film. From the simulation results, SiN waveguides of more than 1.25 μm width are multimode as shown in Fig. 2. Figure 3 shows the fabrication process. The lower cladding layer was formed with a thickness of 1.6 μm by thermal oxidation. Then, 0.9 μm thick SiN was deposited by plasma enhanced chemical vapor deposition. Ring resonators were defined by electron beam lithography and reactive ion etching.

Figure 4 shows the wavelength dependence of optical power of the through port and the drop port for the ring resonators with W = 2.0 μm and g = 0.10 μm. The measured resonance wavelengths agree with theoretical values. Clear subpeaks caused by the second-order mode are not observed; thus, the resonance characteristics of this multimode ring resonator behave similarly to those of the single-mode ring resonator. The reason can be explained as follows. The light field of the second-order mode is more weakly confined than that of the first-order mode in waveguide and so has larger bending loss. An upper limit of waveguide width, however, exists for the ring resonators that do not have subpeaks from the higher-order modes as shown in Fig. 5. The gap dependence of the full width at half maximum (FWHM) of the resonance shape is shown in Fig. 6. The ring resonator with wider gaps has a narrower FWHM.

3. Design and Simulation of Ring Resonator Optical Switches using Electro-Optic Materials

Figure 7 shows ring resonator optical switches using EO materials. We calculated in the case of $LiNbO_3$ (LN), $(Ba,Sr)TiO_3$ (BST), and $K(Ta,Nb)O_3$ (KTN). LN is a widely used for EO material. BST has already been introduced in the Si process as the ferroelectric material [6]. KTN has a very large EO coefficient [7]. We assume the channel structure of the ring waveguide which consists of the EO material core layer and the SiO_2 or KH_2PO_4 (KDP) cladding layer. Then resonance properties of the ring resonator are simulated as shown in Fig. 8. Figure 9 shows the dependence of the operation voltage on the thickness of the core layer for several combinations of core and cladding materials. KTN is promising if a thin film will be available in Si process. LN and BST have high operation voltage. Operation voltage may be reduced by introducing other waveguide structure, such as a ridge type.

The operation speed is estimated using a simple model, which assumes an equivalent index, the coupling constant, and the bending loss [1]. We fix the equivalent index at 2.0 for EO material. Figure 10 shows the resonance shape for a coupling constant of 0.2 after light propagates in the ring for 5, 30, and 100 rounds. Time dependence of peak power and FWHM are shown in Fig 11. The resonance time is estimated to be 15 ps. The operation speed of the ring resonator switches depends on not only resonance time but also the RC delay and polarization times of the EO materials. Typical time is 10^{-2} and 1 ps, respectively. Therefore, the operation speed is limited by the resonance time.

4. Conclusions

We have fabricated multimode ring resonators. For the waveguide width of 2.0 μm, the resonance characteristics behaved similarly to those of single-mode ring resonator. The multimode ring resonators are useful for interconnection on Si chips. We proposed ring resonator optical switches using EO materials, which are promising devices for application to interconnection on Si chips.

References

[1] Y. Tanushi *et al*., Jpn. J. Appl. Phys. **45** (2006) 3493.
[2] A. Liu *et al*., Nature **427** (2004) 615.
[3] T. Naganawa *et al*., Photon. Technol. Lett. **17** (2005) 2104.
[4] Q. Xu *et al*., Nature **435** (2005) 323.
[5] Y. Tanushi *et al*., to be published in Jpn. J. Appl. Phys.
[6] W. Fan *et al*., J. Appl. Phys. **94** (2003) 6192.
[7] S. Toyoda *et al*., Electron. Lett. **40** (2004) 830.

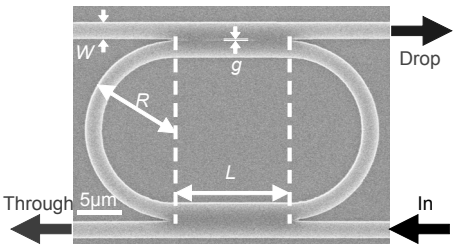

Fig. 1 Structure and parameters of racetrack type resonators. The ring radius R = 10 μm and the coupling length L = 12.56 μm are set to obtain a sufficient large free spectral range of more than 10 nm. The gap is 0.05, 0.10, or 0.15 μm.

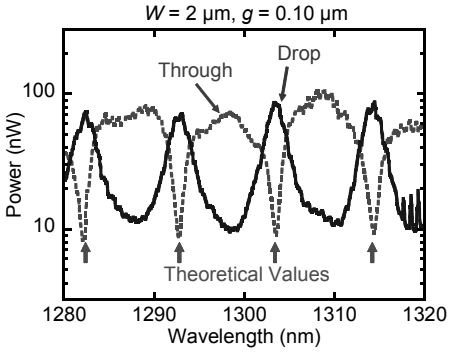

Fig. 4 Wavelength dependence of optical power. The valleys of the through port correspond well to the peaks of the drop port. The measured resonance wavelengths agree with theoretical values. Clear subpeaks caused by the second-order mode are hardly observed.

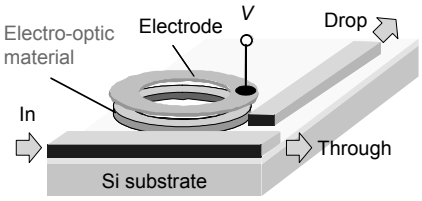

Fig. 7 Ring resonator optical switches using EO materials. In the following simulation, the ring radius and waveguide width are fixed at 12 and 2 μm, respectively.

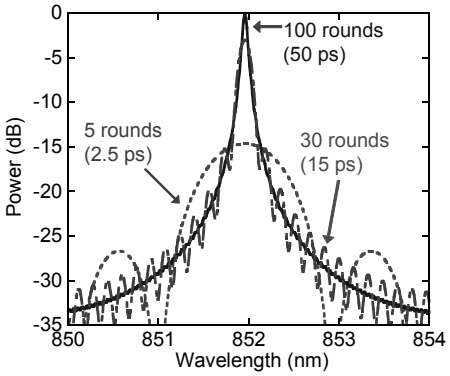

Fig. 10 Time dependence of resonance characteristics for coupling constant of 0.2 and no bending loss.

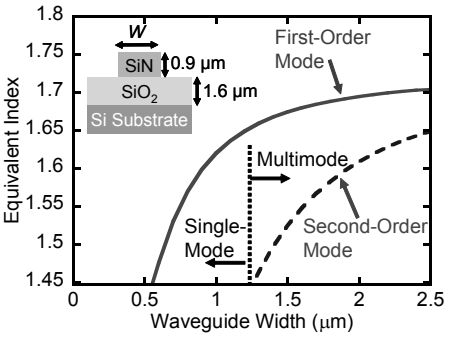

Fig. 2 Waveguide width dependence of equivalent index at λ = 1.3 μm by simulation. The refractive index of SiN and SiO_2 are 1.80 and 1.447, respectively.

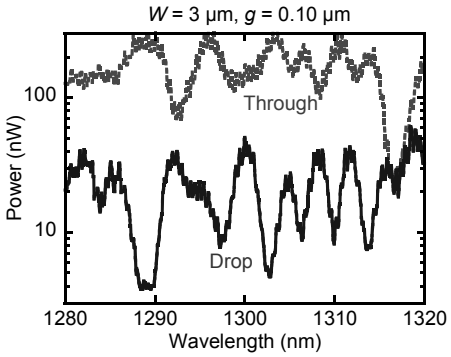

Fig. 5 Wavelength dependence of optical power. Subpeaks caused by the higher-order modes are observed.

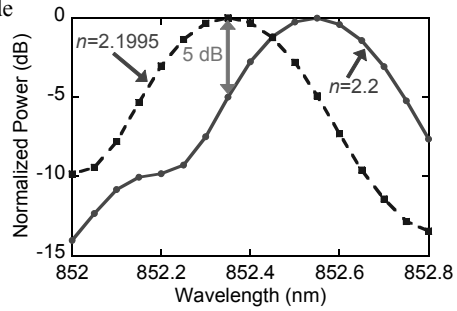

Fig. 8 Simulated resonance properties for different refractive indices of the core. Refractive index change of $5x10^{-4}$ is needed for switching operation with switching gain of 5 dB.

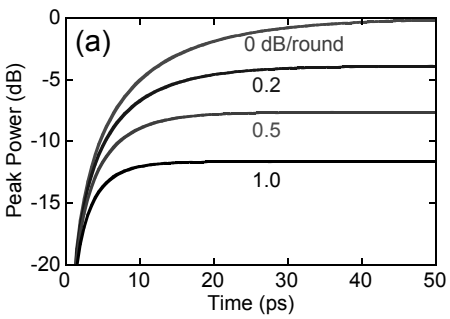

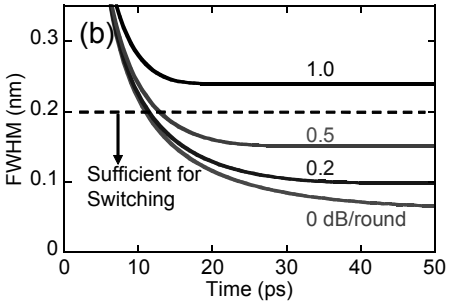

Fig. 11 Time dependence of (a) peak power and (b) FWHM for coupling constant of 0.2. It takes less than 15 ps to reach FWHM of 0.2 nm when bending loss is sufficiently small.

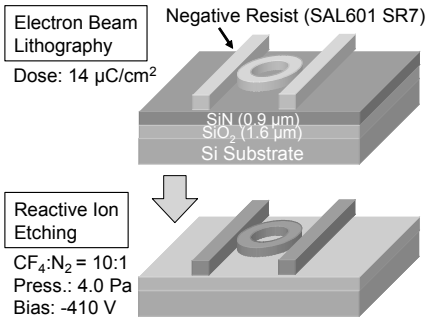

Fig. 3 Fabrication process of ring resonators.

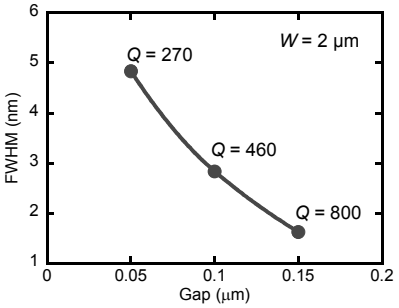

Fig. 6 Gap dependence of the FWHM of the resonance shape. The ring resonator with wider gaps has a narrower FWHM.

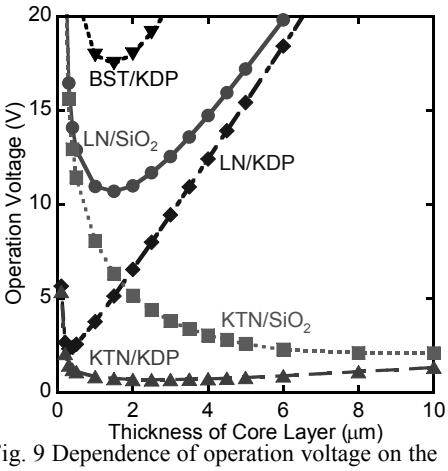

Fig. 9 Dependence of operation voltage on the core thickness for various combinations of core and cladding materials. The operation voltage depends on thicknesses of both core and cladding layers. The cladding layer thickness is chosen such that the propagation loss becomes less than 1.0 dB/cm.